Narrowband Internet of Things: Repetition-Based Coverage Performance Analysis of Uplink Systems

Md Sadek Ali, Yu Li, Song Chen, and Fujiang Lin
Micro-/Nano-Electronic System Integration R&D Center (MESIC), Department of Electronic Science and Technology, University of Science and Technology of China (USTC), Hefei, Anhui, 230027, PR China
Email: sadek@mail.ustc.edu.cn; yuli1@mail.ustc.edu.cn; songch@ustc.edu.cn; linfj@ustc.edu.cn

Abstract —A novel narrowband and low-power wide area network (LPWAN) technology named Narrowband Internet of Things (NB-IoT) based on Long Term Evolution (LTE) has been standardized by 3rd Generation Partnership Project (3GPP) in Release-13 to provide massive connectivity for Internet of Things (IoT). In NB-IoT systems, repeating same signal over additional period of time has been taken as a key technique to enhance radio coverage up to 20 dB compared to the legacy General Packet Radio Service (GPRS). NB-IoT system modeling and optimization of system performance is still challenging particularly coverage improvement in the case of practical applications. In this paper, we develop a repetition-dominated system model and evaluate the link-level coverage performance of NB-IoT uplink systems. Coverage performance based on signal repetition is also depended on the channel estimation accuracy. Besides, narrowband demodulation reference signal (NDMRS) assisted channel estimation and frequency-domain equalization are exploited on the receiver side. Link-level extensive simulations are performed to validate the uplink coverage performance for both single-tone and multi-tone transmissions. The results show that our proposed system model with repetition-dominated approach guarantees the transmission reliability in worse channel conditions of NB-IoT uplink systems as well as enhance the radio coverage.

Index Terms—Least Square (LS) estimation, Machine-to-Machine (M2M) communications, narrowband internet of things (NB-IoT), Resource Unit (RU), repetitions, Single Carrier Frequency Division Multiple Access (SC-FDMA), Zero Forcing (ZF) equalization.

I. Introduction

Internet of Things (IoT) is the network of physical objects such as devices, vehicles, Radio-Frequency Identification (RFID) tags, sensors, and consumer-electronics that are connected to the internet through embedded devices and software. Nowadays, IoT is one of the important strategic industries in the world. The massive number of connected IoT devices is growing to enable the future Fifth Generation (5G) wireless communication systems. Ericsson predicts that there will be around 28 billion connected devices by 2021, of which more than 15 billion will be connected Machine-to-Machine (M2M) and consumer-electronics devices [1]. According to Nokia [2] based on Machina research 2015, an estimated 30 billion connected devices will be deployed by 2025, of which cellular IoT and low-power wide area (LPWA) modules are around 23%. Increasing number of smart devices and connections as those having advanced computing and multimedia capabilities that requires more capable and intelligent networks. On the other hand, LPWA connections specifically for M2M and consumer-electronics devices those need narrow bandwidth, wide geographic coverage, and low delay sensitivity [3].

Connectivity is the main objective of IoT, and the type of access required will be depended on the nature of applications. However, a significant share of devices will be served by short-range (e.g., tens or hundreds of meters) radio technologies such as Wi-Fi, Bluethooth low energy (BLE), ZigBee, Z-Wave, and so forth [4], [5]. There are a number of LPWA technologies allow devices to be connected to the internet that operate in unlicensed spectrum such as SigFox [6], and LoRa [7] and licensed band such as Global System for Mobile Communication (GSM), and 3rd Generation Partnership Project (3GPP) standard Long Term Evolution (LTE) with very limited demands on throughput and reliability. On the GSM side the so called Extended Coverage GSM (EC-GSM) standard was released whereas on the LTE side two new device categories were standardized in Release-13: LTE Cat-M1 and LTE Cat-NB1 also called Narrowband Internet of Things (NB-IoT) [8]. Both new LTE categories reduce the communication bandwidth from 20 MHz (LTE Cat-1) to 1.4 MHz for Cat-M1 and to 200 kHz for Cat-NB1 [9], [10]. Among these technologies, NB-IoT is designed as a key enabling technology specifically for ultra-low-throughput IoT applications. NB-IoT has a wide range of use cases in the future can be categorized as smart metering, smart cities, smart buildings, agriculture and environment, consumer, and so on. The motivation behind the new standard was designed to enable energy efficient operation of communication devices while reducing their cost and extending their coverage range. To meet the extremely demanding low energy requirements of IoT applications, the 3GPP specifications target devices with ten years of battery life. Study item regarding NB-IoT was created to attain the performance objectives [11], [12]: improved

Manuscript received January 3, 2018; revised May 12, 2018.
The first author is sponsored by the CAS-TWAS President's Fellowship Program.
*Corresponding author email: songch@ustc.edu.cn.
doi:10.12720/jcm.13.6.293-302

indoor coverage, support massive number of low-throughput devices, ultra-low-cost and complexity devices, improved power efficiency, and low delay sensitivity. Despite it being a key enabling technology for IoT, NB-IoT system modeling and optimization of system performance is still challenging particularly coverage enhancement. According to the specifications of 3GPP in Release-13, repetition of user data has been taken as a key technique to enhance coverage and improve transmission reliability. Although large number of same signal repetition enhances coverage but reduces spectral efficiency.

Since NB-IoT is still in its infancy, coverage analysis research is rather limited in current literature. In literature, most of the NB-IoT research focuses on frame structure design [11], scheduling and link adaptation [13], equalization and interference analysis [14], and system acquisition [15]. M. Lauridsen *et al*. [16] presented coverage comparison of GPRS, NB-IoT, LoRa, and SigFox in a 7800 Km^2 area. The authors showed that NB-IoT provides best coverage among four technologies. R. Ratasuk *et al*. [17] studied uplink and downlink data channel design and its performance for LTE NB-IoT. In [18], the authors evaluated the performance of different channel estimation algorithms for NB-IoT uplink systems. A. Adhikary *et al*. [19] evaluated the coverage performance of NB-IoT systems. This is the first time that a coverage performance was evaluated for both uplink and downlink. For the uplink only single-tone transmission was taken into account for evaluation. However, our study is entirely different from this work. To the best of our knowledge, coverage performance of NB-IoT uplink for multi-tone transmission has not been investigated yet.

In this paper, we focus on developing a novel LTE-based repetition-dominated NB-IoT uplink system model to evaluate the link-level coverage performance for both single-tone and multi-tone transmissions. We focus on uplink because uplink transmission of NB-IoT system is more complicated than downlink transmission. The major contribution of this paper can be summarized as follows:

1. We provide a brief overview of NB-IoT systems including deployment options, multiple access schemes, and uplink resource unit (RU) definition. An analytic repetition-dominated NB-IoT uplink baseband signal model including narrowband demodulation reference signal (NDMRS) is derived based on our proposed system model. The purpose of signal repetition is to ensure the transmission reliability (i. e., block error rate (BLER) <10%) at low signal-to noise ratio (SNR) condition.
2. We analyze NDMRS-based channel estimation and frequency-domain equalization (FDE) to combat multipath fading effect at the receiver. Least Square (LS) estimation and Zero Forcing (ZF) equalization are employed.
3. Extensive computer simulations are performed to validate the link-level coverage performance of repetition-dominated NB-IoT uplink systems. The simulation results indicate that the radio coverage can be enhanced up to 20 dB compared to legacy LTE technology.

The rest of the paper is organized as follows. In section II, a brief overview of NB-IoT systems is provided. Repetition-dominated NB-IoT uplink signal model is derived in section III. In section IV, theoretical analysis of channel estimation and frequency-domain equalization are provided. Simulation results and analysis are presented in section V. Finally, concludes the paper in section VI.

Notations: Bold face lower-case (upper-case) letters are used to represent (time/frequency-domain) vectors and matrices, respectively. Superscripts $(\cdot)^T$ and $(\cdot)^H$ denote the transpose and Hermitian of a vector, a scalar, or a matrix respectively and $(\cdot)^{-1}$ denotes matrix inversion. The operator * and $|\cdot|$ denote the convolution operation and the absolute value respectively.

II. Overview of NB-IoT Systems

NB-IoT is a new radio interface technology which occupies system bandwidth of 180 KHz for both uplink and downlink with half duplex frequency division duplexing (FDD). There are three deployment options defined by 3GPP standard such as stand-alone, in-band, and guard-band [20]. In stand-alone case, NB-IoT can be used one or more efficiently re-framed 200 KHz GSM carriers. For the in-band and guard-band deployment, NB-IoT supports most of the LTE functionalities with some simplification [21]. It therefore uses 180 KHz bandwidth, which corresponds to one physical resource block (PRB) of LTE transmission for in-band. It utilizes unused resource blocks within an LTE carrier's guard-band for guard-band deployment. The three deployment scenario of NB-IoT is shown in Fig. 1.

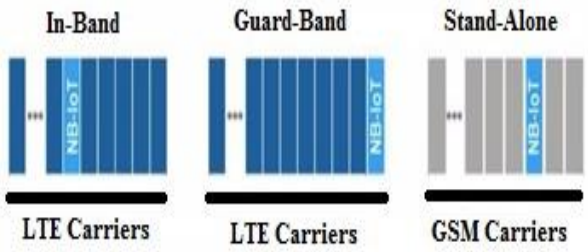

Fig. 1. NB-IoT deployment options.

In the downlink, NB-IoT completely allows downlink numerology from existing LTE technology. Thus, orthogonal frequency division multiplexing (OFDM) with 15 KHz sub-carrier spacing is used in the downlink. For baseband modulation in NB-IoT uplink two different schemes are possible [22]: multi-tone transmission is according to single-carrier frequency division multiple access (SC-FDMA) and single-tone transmission (FDMA). Both schemes are based on the separation of the available spectrum into orthogonal subcarriers, each

of which is then used to transfer a stream of data. In the case of SC-FDMA, multiple subcarriers are simultaneously used by the same user while for single-tone transmissions each user only uses one subcarrier at a time. For single-tone transmission, two different subcarrier spacing are possible: 15 kHz and 3.75 kHz. The first one is the same as LTE standard and leads to a total of 12 subcarriers whereas the second one leads to a total of 48 subcarriers. Multi-tone transmissions can only use the 15 kHz subcarrier spacing [22].

TABLE I: NPUSCH RESOURCE UNIT (RU) FORMAT

Subcarrier spacing	No. of subcarriers	No. of slots	No. of SC-FDMA symbols
3.75 KHz	1	16	112
15 KHz	1	16	112
	3	8	56
	6	4	28
	12	2	14

Repetitions of user data block over a specified number of slots is the key technique allowed for NB-IoT to achieve deep penetration in excessive bad radio conditions. In the case of Narrowband Physical Uplink Shared Channel (NPUSCH) repetitions, the number of repetitions depends on the coverage enhancement level needed by low-end IoT devices [23]. However, repetitions for NPUSCH transmission can only be chosen from the set {1, 2, 4, 8, 16, 32, 64, 128}, where the numerical value indicates the repetition number of the same transport block. The 3GPP [22], introduces a new concept for NB-IoT uplink systems called Resource Unit (RU) as a basic unit for NPUSCH allocation. The Table I shows the characterization of NPUSCH resource unit. In 3GPP [23] defined the Transport Block Size (TBS) with different number of RUs where TBS index represents the Modulation and Coding Scheme (MCS) level. The maximum supported TBS is 1000 bits in Release-13 of the NB-IoT specification.

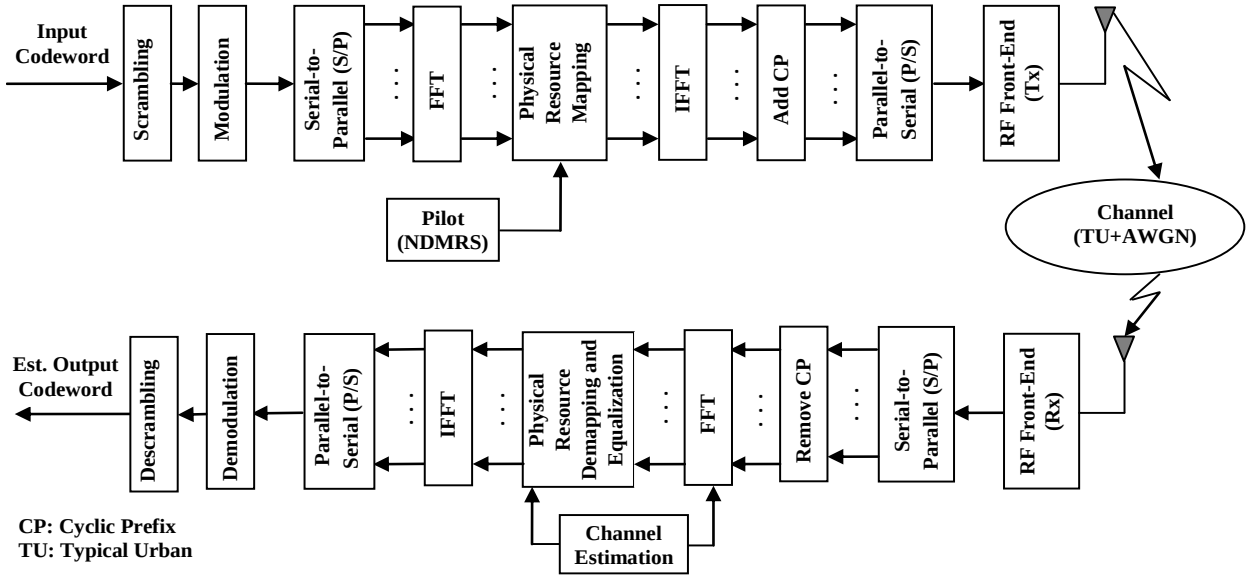

Fig. 2. Block diagram of NB-IoT uplink system model.

III. NB-IOT UPLINK SYSTEM MODEL

The proposed system model of NB-IoT uplink with channels, reference signal sequence, and the associated estimation and equalization blocks is shown in Fig. 2. The baseband signal processing in the transmitter of an uplink system is a combination of transport channel which is also known as uplink shared channel (UL-SCH) and data channel (NPUSCH) processing. Binary information arrives to the channel coding unit in the form of one TBS over a number of RUs. The number of resource unit is scheduled according to [23]. In UL-SCH processing [24], we perform transport block Cyclic Redundancy Check (CRC) attachment (e. g., 24 bits with generator polynomial $g_{CRC24A}(D)$), turbo coding based on a 1/3-rate code, and rate matching to generate a codeword input to the NPUSCH. We assume that for a single codeword transmission, a block of N_{bit} transmitted bits $\mathbf{b} = [b(1), b(2), \ldots, b(N_{\text{bit}} - 1)]^{\text{T}}$ drawn from the output of the channel coding. The codeword bits **b** are scrambled with the NB-IoT user equipment (NB-IoT UE) specific scrambling sequence. The output $\tilde{b}(i)$ can be expressed as

$$\tilde{b}(i) = (b(i) + c(i)) \bmod 2 \tag{1}$$

where $i = 0,1,\ldots,N_{\text{bit}} - 1$, and $c(i)$ is the scrambling sequence defined by a length-31 Gold sequence [22]. The initialization value of the first sequence is specified with a unit impulse function of length-31. The second scrambling sequence can be initialized with

$$c_{\text{init}} = n_{\text{RNTI}} \cdot 2^{14} + n_f \bmod 2 \cdot 2^{13} + \lfloor n_s / 2 \rfloor \cdot 2^9 + N_{\text{ID}}^{\text{Ncell}} \tag{2}$$

where n_{RNTI} denotes the index of radio network temporary identifier (RNTI), n_s is the first slot index of

the transmission of the codeword, and $N_{\mathrm{ID}}^{\mathrm{Ncell}}$ is the narrowband physical cell identity number. For the repetitions of NPUSCH, the scrambling sequence will be reinitialized according to (2) after every $N_{\mathrm{identical}}^{\mathrm{NPUSCH}}$ (i. e., same signal) transmission with n_{s} and n_f set to the first slot and the frame respectively.

The block of bits $\tilde{b}(i)$ are modulated by exploiting NB-IoT supported modulation schemes (e. g., $\pi/2$ - BPSK, and $\pi/4$ -QPSK) and yielding a block of complex-valued symbols $\mathbf{s}=[s(0),s(1),\ldots,s(N_{\mathrm{symb}}-1)]^{\mathrm{T}}$, where N_{symb} represents the number of modulated symbols. The block of modulation symbols $\mathbf{s}$ is divided into $N_{\mathrm{symb}}/M_{\mathrm{sc}}^{\mathrm{NPUSCH}}$ groups, each corresponding to one SC-FDMA symbol. The quantity $M_{\mathrm{sc}}^{\mathrm{NPUSCH}}=N_{\mathrm{RB}}^{\mathrm{NPUSCH}}.N_{sc}^{\mathrm{RB}}$ represents the number of scheduled subcarriers for NPUSCH transmission, where $N_{\mathrm{RB}}^{\mathrm{NPUSCH}}$ denotes the bandwidth of NPUSCH in terms of PRB, and $N_{\mathrm{sc}}^{\mathrm{RB}}$ is the number of subcarriers in a PRB. The modulation constellation is transformed into frequency-domain by means of discrete Fourier transform (DFT) as

$$X(l\cdot M_{\mathrm{sc}}^{\mathrm{NPUSCH}}+k)=\frac{1}{\sqrt{M_{\mathrm{sc}}^{\mathrm{NPUSCH}}}}\sum_{i=0}^{M_{\mathrm{sc}}^{\mathrm{NPUSCH}}-1}s(l\cdot M_{\mathrm{sc}}^{\mathrm{NPUSCH}}+i)e^{-j\frac{2\pi ik}{M_{\mathrm{sc}}^{\mathrm{NPUSCH}}}},\quad 0\le k\le M_{\mathrm{sc}}^{\mathrm{NPUSCH}}-1,\quad 0\le l\le N_{\mathrm{symb}}/M_{\mathrm{sc}}^{\mathrm{NPUSCH}}-1 \tag{3}$$

yielding a block of frequency-domain symbols $\mathbf{x}=[x(0),x(1),\ldots,x(N_{\mathrm{symb}}-1)]^{\mathrm{T}}$.

In NB-IoT uplink systems, known reference pilot symbols also known as NDMRS are multiplexed together with the user data symbols to estimate channel impulse response (CIR). A NDMRS sequence $\mathbf{d}_u(n)$ for number of subcarriers in a resource unit $N_{\mathrm{sc}}^{\mathrm{RU}}=1$ can be defined as

$$\mathbf{d}_u(n)=\frac{1}{\sqrt{2}}(1+j)(1-2c(n))w(n\bmod 16),\quad 0\le n<R_{\mathrm{rep}}^{\mathrm{NPUSCH}}N_{\mathrm{slots}}^{\mathrm{UL}}N_{\mathrm{RU}} \tag{4}$$

where $c(n)$ is the binary sequence defined by a length-31 Gold sequence, $R_{\mathrm{rep}}^{\mathrm{NPUSCH}}$ denotes the repetition number of the same signal, $N_{\mathrm{slots}}^{\mathrm{UL}}$ represents number of uplink slots, and N_{RU} is the number of resource units. The initialization value of the first sequence is specified with a unit impulse function of length-31. The initialization of the second sequence is denoted $c_{\mathrm{init}}=35$ at the start of the NPUSCH transmission [22]. The quantity $w(n)$ is defined in [22] where the base sequence index $u=N_{\mathrm{ID}}^{\mathrm{Ncell}}\bmod 16$ for NPUSCH format-1 without enabling group hopping. Thus, the NDMRS sequence $d_u(n)$ for NPUSCH format-1 can be written as

$$d_u(n)=\mathbf{d}_{\mathbf{u}}(n). \tag{5}$$

The NDMRS sequence $d_u(n)$ for number of subcarriers greater than one in a RU is defined by a cyclic shift α of a base sequence as

$$d_u(n)=e^{j\alpha n}e^{j\varphi(n)\pi/4},0\le n\le N_{\mathrm{sc}}^{\mathrm{RU}} \tag{6}$$

where $\varphi(n)$ is defined in [22] for the scheduled number of subcarriers in a RU. We assume that there is no higher layer signaling, the base sequence index u can be obtained as

$$u=\begin{cases}N_{\mathrm{ID}}^{\mathrm{Ncell}}\bmod 12 & \text{for } N_{\mathrm{sc}}^{\mathrm{RU}}=3\\ N_{\mathrm{ID}}^{\mathrm{Ncell}}\bmod 14 & \text{for } N_{\mathrm{sc}}^{\mathrm{RU}}=6\\ N_{\mathrm{ID}}^{\mathrm{Ncell}}\bmod 30 & \text{for } N_{\mathrm{sc}}^{\mathrm{RU}}=12\end{cases}. \tag{7}$$

The cyclic shift α for $N_{\mathrm{sc}}^{\mathrm{RU}}=3$ and 6 is defined in [22]. For $N_{\mathrm{sc}}^{\mathrm{RU}}=12$, $\alpha=0$.

The physical resource element mapping is performed by placing frequency-domain symbols within the resource grid. NPUSCH can be mapped to one or more than one RU according to [23], each of which can be transmitted $R_{\mathrm{rep}}^{\mathrm{NPUSCH}}$ times. The block of frequency-domain symbols $\boldsymbol{X}$ are mapped in sequence (i. e., localized mapping) to subcarriers assigned for transmission [22], [25]-[27]. The mapping to resource elements (k,l) will be accomplished at the first slot in the assigned RU in increasing order of the first subcarrier index k, then the symbol index l and finally the slot number. After mapping to N_{slots} slots, the N_{slots} repeats $N_{\mathrm{identical}}^{\mathrm{NPUSCH}}$ additional times, before continuing the mapping of $\boldsymbol{X}(\cdot)$ to the following slot. The variable $N_{\mathrm{identical}}^{\mathrm{NPUSCH}}$ can be defined as

$$N_{\mathrm{identical}}^{\mathrm{NPUSCH}}=\begin{cases}\min\left(\left\lceil R_{\mathrm{rep}}^{\mathrm{NPUSCH}}/2\right\rceil,4\right) & N_{\mathrm{sc}}^{\mathrm{RU}}>1\\ 1 & N_{\mathrm{sc}}^{\mathrm{RU}}=1\end{cases} \tag{8}$$

$$N_{\mathrm{slots}}=\begin{cases}1 & \Delta f=3.75\,\mathrm{kHz}\\ 2 & \Delta f=15\,\mathrm{kHz}\end{cases} \tag{9}$$

where, Δf denotes subcarrier spacing. The mapping of $\mathbf{x}$ is then repeated until $R_{\mathrm{rep}}^{\mathrm{NPUSCH}}N_{\mathrm{RU}}N_{\mathrm{slots}}^{\mathrm{UL}}$ slots have been transmitted.

In each NB-IoT uplink slots, NDMRS are mapped in scheduled number of subcarriers in a RU of the fourth SC-FDMA symbols for 15 KHz subcarrier spacing whereas the fifth symbol for 3.75 KHz subcarrier spacing. Fig. 3 shows, for example, the NB-IoT uplink resource grid mapping of NPUSCH format-1 including NDMRS, where a RU contains 12 subcarriers for 15 KHz subcarrier spacing and only one subcarrier for 3.75 subcarrier spacing.

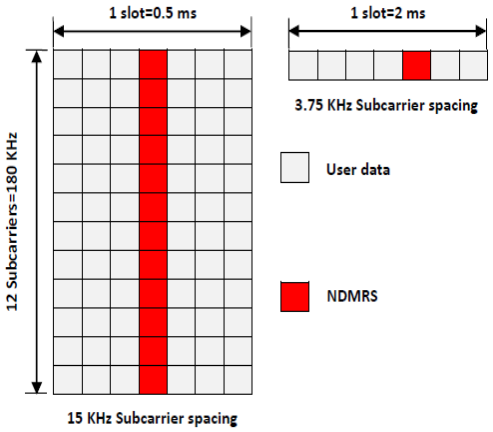

Fig. 3. NB-IoT uplink resource grid mapping.

The physical resource element mapping is followed by an inverse discrete Fourier transform (IDFT) to convert the data into time-domain signal. After the Cyclic Prefix insertion of length $N_{\mathrm{CP},l}$, the time-domain signal $y_l(t)$ in SC-FDMA symbol $l \in \{0,1,\ldots,6\}$ in an uplink slot for multi-tone transmission can be written as

$$y_l(t) = \sum_{k=-\lfloor N_{\mathrm{sc}}^{\mathrm{RU}}/2 \rfloor}^{\lceil N_{\mathrm{sc}}^{\mathrm{RU}}/2 \rceil - 1} a_{k^{(-)},l} \cdot e^{j2\pi(k+1/2)\Delta f\left(t - N_{\mathrm{CP},l} T_{\mathrm{s}}\right)} \tag{10}$$

for $0 \le t < \left(N_{\mathrm{CP},l} + N\right) \times T_{\mathrm{s}}$ where $k^{(-)} = k + \lfloor N_{\mathrm{sc}}^{\mathrm{RU}}/2 \rfloor$, $N = 2048$, $\Delta f = 15\,\mathrm{kHz}$, T_{s} is the basic time unit specified for NB-IoT as a factor of $T_{\mathrm{s}} = 1/(15000 \times 2048)$ seconds, and $a_{k,l}$ is the content of resource element (k,l). Note that only normal CP length $N_{\mathrm{CP},l}$ of existing LTE is supported in Release-13 of the NB-IoT specification.

For single-tone transmission, the time-domain signal $y_{k,l}(t)$ for the k-th subcarrier in SC-FDMA symbol l in an uplink slot can be represented as

$$\begin{aligned} y_{k,l} &= a_{k^{(-)},l} \cdot e^{j\varphi_{k,l}} \cdot e^{j2\pi(k+1/2)\Delta f\,(t - N_{\mathrm{cp},l} T_{\mathrm{s}})} \\ k^{(-)} &= k + \lfloor N_{\mathrm{sc}}^{\mathrm{RU}}/2 \rfloor \end{aligned} \tag{11}$$

for $0 \le t < \left(N_{\mathrm{CP},l} + N\right) T_{\mathrm{s}}$ where parameters for $\Delta f = 15\,\mathrm{kHz}$ and $\Delta f = 3.75\,\mathrm{kHz}$ are given in Table II, $a_{k^{(-)},l}$ is the modulation value of symbol l and the phase rotation $\varphi_{k,l}$ is defined according to [22]

TABLE II: SC-FDMA PARAMETERS FOR $N_{\mathrm{sc}}^{\mathrm{RU}} = 1$

Parameter	Subcarrier spacing	
	3.75 KHz	15 KHz
N	8192	2048
Cyclic prefix length $N_{\mathrm{CP},l}$	256	160 for $l = 0$ 144 for $l = 1,2,\ldots,6$
Set of values for k	-24,-23,…,23	-6,-5,…,5

$$\begin{aligned} \varphi_{k,l} &= \rho\left(\tilde{l} \bmod 2\right) + \hat{\varphi}_k\left(\tilde{l}\right) \\ \rho &= \begin{cases} \frac{\pi}{2} & \text{for BPSK} \\ \frac{\pi}{4} & \text{for QPSK} \end{cases} \\ \hat{\varphi}_k\left(\tilde{l}\right) &= \begin{cases} 0 & \tilde{l} = 0 \\ \hat{\varphi}_k\left(\tilde{l} - 1\right) + 2\pi\Delta f\left(k + 1/2\right)\left(N + N_{CP,l}\right)T_{\mathrm{s}} & \tilde{l} > 0 \end{cases} \\ \tilde{l} &= 0,1,\ldots,R_{\mathrm{rep}}^{\mathrm{NPUSCH}} N_{\mathrm{RU}} N_{\mathrm{slots}}^{\mathrm{UL}} N_{\mathrm{symb}}^{\mathrm{UL}} - 1 \\ l &= \tilde{l} \bmod N_{\mathrm{symb}}^{\mathrm{UL}} \end{aligned} \tag{12}$$

where $\tilde{l}$ is the symbol counter that is reset at the start of a transmission and incremented for each symbol during the time of transmission.

The time-domain baseband signal is upconverted by a RF front-end and then propagates through a multipath fading channel whose delay speared is considered to be smaller than the CP length. The received signal for both multi-tone and single-tone transmission is composed of the signals from different channel paths and additive noise which can be modeled as the convolution of transmitted signal and CIR

$$r_{\text{M-tone}}(t) = y_l(t) * h(t) + w(t) \tag{13}$$

$$r_{\text{S-tone}}(t) = y_{k,l}(t) * h(t) + w(t) \tag{14}$$

where $w(t)$ is the Additive White Gaussian Noise (AWGN) with zero mean and noise variance σ^2, $r_{\text{M-tone}}(t)$ and $r_{\text{S-tone}}(t)$ represents the received signal for multi-tone and single-tone transmission respectively, and $h(t)$ denotes the CIR of the multipath fading channel with a finite number of L distinct taps can be expressed as

$$h(t) = \sum_{i=0}^{L-1} \beta_i \delta(t - \tau_i) \tag{15}$$

where β_i and τ_i represents the attenuation and the delay of the i-th path respectively. Hence, the distorted and delayed version of the received signal can be written as

$$r_{\text{M-tone}}(t) = \sum_{i=0}^{L-1} \beta_i y_l(t - \tau_i) + w(t) \tag{16}$$

$$r_{\text{S-tone}}(t) = \sum_{i=0}^{L-1} \beta_i y_{k,l}(t - \tau_i) + w(t)\,. \tag{17}$$

After removing CP, the receiver performs inverse operations of the NPUSCH and the UL-SCH processing including NDMRS assisted channel estimation and frequency-domain equalization which are described in section IV.

IV. CHANNEL ESTIMATION AND EQUALIZATION

Channel estimation is performed based on the known NDMRS symbols. This can be accomplished by using Least Square (LS) algorithm, which is one-dimensional (1D) estimator. We assume that all the subcarriers $N_{\mathrm{sc}}^{\mathrm{RU}}$

in a RU are occupied by pilot symbols, and we arrange $\mathbf{p}$ as a group of pilot symbols for $N_{\text{sc}}^{\text{RU}}$ subcarriers as

$$\mathbf{p} = [\,p(0) \quad p(1) \quad \ldots \quad p(N_{\text{sc}}^{\text{RU}} - 1)]^T . \tag{18}$$

Let $\mathbf{P}$ is a $N_{\text{sc}}^{\text{RU}} \times N_{\text{sc}}^{\text{RU}}$ matrix with elements of $\mathbf{p}$ on its diagonal can be expressed as

$$\mathbf{P} = \begin{bmatrix} p(0) & \cdots & 0 \\ \vdots & \ddots & \vdots \\ 0 & \cdots & p(N_{\text{sc}}^{\text{RU}} - 1) \end{bmatrix}. \tag{19}$$

The LS channel estimator estimates the channel impulse response $\hat{\mathbf{h}}_{\text{LS}}$ by minimizing the square error ε as

$$\varepsilon = \left| \mathbf{y} - \mathbf{P}\mathbf{W}_{N_{\text{sc}}^{\text{RU}}} \hat{\mathbf{h}}_{\text{LS}} \right|^2 \tag{20}$$

and

$$\hat{\mathbf{h}}_{\text{LS}} = \arg_{\hat{\mathbf{h}}_{\text{LS}}} \min(\mathbf{y} - \mathbf{P}\mathbf{W}_{N_{\text{sc}}^{\text{RU}}} \hat{\mathbf{h}}_{\text{LS}})^{\text{H}} (\mathbf{y} - \mathbf{P}\mathbf{W}_{N_{\text{sc}}^{\text{RU}}} \hat{\mathbf{h}}_{\text{LS}}) \tag{21}$$

where $\mathbf{W}_{N_{\text{sc}}^{\text{RU}}}$ is the $N_{\text{sc}}^{\text{RU}} \times N_{\text{sc}}^{\text{RU}}$ DFT matrix, and $\mathbf{y}$ is the received vector which has the dimension $N_{\text{sc}}^{\text{RU}} \times 1$. The estimated channel impulse response that minimizes ε as

$$\hat{\mathbf{h}}_{\text{LS}} = \mathbf{M}\mathbf{W}_{N_{\text{sc}}^{\text{RU}}}^{\text{H}} \mathbf{P}^{\text{H}} \mathbf{y} \tag{22}$$

where

$$\mathbf{M} = (\mathbf{W}_{N_{\text{sc}}^{\text{RU}}}^{\text{H}} \mathbf{P}^{\text{H}} \mathbf{P} W_{N_{\text{sc}}^{\text{RU}}})^{-1}. \tag{23}$$

The frequency-domain representation of (22) can be expressed as

$$\begin{aligned} \hat{\mathbf{H}}_{\text{LS}} &= \mathbf{W}_{N_{\text{sc}}^{\text{RU}}} \hat{\mathbf{h}}_{\text{LS}} \\ &= \mathbf{W}_{N_{\text{sc}}^{\text{RU}}} \mathbf{M}\mathbf{W}_{N_{\text{sc}}^{\text{RU}}}^{\text{H}} \mathbf{P}^{\text{H}} \mathbf{y} \end{aligned}. \tag{24}$$

Finally, from (23) and (24), the channel impulse response can be estimated as

$$\hat{\mathbf{H}}_{\text{LS}} = \mathbf{P}^{-1}\mathbf{y} \tag{25}$$

where $\mathbf{P}$ contains only the pilot symbols and $\mathbf{y}$ represents received pilot symbols excluding data symbols. Thus, the LS estimation estimates the channel impulse response in frequency-domain by simply dividing the received pilots by the known transmitted pilots. The channel impulse responses for the remaining SC-FDMA symbols of the resource grid are estimated by using 1D time-domain interpolation.

The equalizer gain in frequency-domain can be computed by means of Zero-Forcing (ZF) algorithm as

$$\mathbf{H}_{\text{ZF}} = \frac{\mathbf{y}}{\hat{\mathbf{H}}_{\text{LS}}} \tag{26}$$

where $\mathbf{y}$ represents received pilot symbols and $\hat{\mathbf{H}}_{\text{LS}}$ denotes the frequency-domain channel impulse response estimated by LS algorithm. ZF is the simplest algorithm, in which the gain is found as the ratio of the resource element to the estimated channel at each subcarrier.

V. Simulation Results and Analysis

We consider LTE-based NB-IoT uplink systems according to block diagram as shown in Fig. 2 to evaluate the link-level coverage performance of NPUSCH format-1. To evaluate the achievable coverage performance through computer simulations, we set the fundamental parameters as listed in Table III and referred to figure captions for better understanding. In this case, we consider a simple single-input single-output (SISO) system for both single-tone with 15 KHz and 3.75 KHz subcarrier spacing and multi-tone transmissions. Link performance is evaluated under Typical Urban (TU) channel and Doppler of 1 Hz.

Table III: Simulation Parameters

Parameter	Value
System bandwidth	180 KHz
Carrier bandwidth	900 MHz
Subcarrier spacing	15 KHz, 3.75 KHz
Transmission mode	Singe-tone, multi-tone(3, 6, and 12)
Channel coding	Turbo(1/3-coding rate)
Modulation schemes	BPSK, QPSK
CRC	24 bits
Antenna configuration	SISO (1Tx×1Rx)
Propagation channel	TU, f_d=1 Hz
Channel estimation	LS (NDMRS-based)
Equalization	Zero Forcing
Number of iterations	10^5
Simulation tool	MATLAB (R2016b)

Simulation results of the performance for our proposed repetition-dominated system by employing both $\pi/2$ -BPSK, and $\pi/4$ -QPSK modulations with different simulation settings for single-tone transmission are shown in Fig. 4 and Fig. 5. We set the repetition number to make sure the transmission reliability (i. e., BLER < 10 percent) at low SNR. As shown in Fig. 4, we compare the performance of NPUSCH between 15 KHz and 3.75 KHz subcarrier spacing for same transmission time and resources. Transmission time and resource utilization are the main objective in our coverage investigation because small transmission time and high rate of resource utilization can enhance the data rate of NB-IoT systems. The results indicate that the BLER increases with as the receive SNR decreases (i. e., worse channel condition). For RU=10 as shown in Fig. 5, coverage performance is slightly less than or equal to the performance of RU=1 due to same transmission time. Furthermore, coverage performance with the 15 KHz subcarrier spacing is always better than the 3.75 KHz subcarrier spacing in any repetition. Performance results for single-tone transmission are summarized in Table IV.

Fig. 6 shows the coverage investigation of NPUSCH for multi-tone transmission by exploiting QPSK modulation scheme. The simulation result shows that the coverage performance increases with as the subcarrier and repetition number increases. The summery of our investigations for multi-tone transmission are given in Table V.

TABLE IV: PERFORMANCE OF NPUSCH FOR SINGLE-TONE TRANSMISSION

Subcarrier spacing	Modula-tion	MCS	Tx- time (ms)	Repetition	SNR (dB) (BLER=10^{-1})	
					RU=1	RU=10
15 KHz	BPSK	0	32	4	7	6
		0	512	64	-3.6	-2.4
	QPSK	4	32	4	10	13
		4	512	64	-2.4	-2.2
3.75 KHz	BPSK	0	32	1	10	14
		0	512	16	-2.4	-1
	QPSK	4	32	1	12	14.5
		4	512	16	-1.2	-1

TABLE V: PERFORMANCE OF NPUSCH FOR MULTI-TONE TRANSMISSION

No. of Subcarriers	Modula-tion	MCS	Tx- time (ms)	Repetition	SNR (dB) (BLER=10^{-1}) RU=1
3	QPSK	4	4	1	12.5
		4	128	32	-1
6		4	4	2	10
		4	128	64	-2.5
12		4	4	4	6
		4	128	128	-3.2

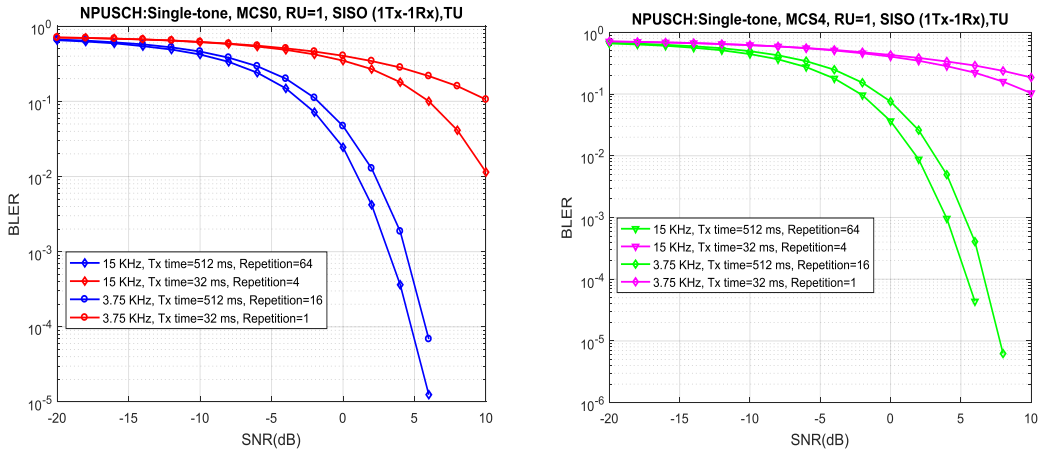

(a) (b)

Fig. 4. BLER performance of NPUSCH with single-tone transmission for both 15 KHz and 3.75 KHz subcarrier spacing using repetitions. Resource unit RU=1. (a) $\pi/2$ -BPSK , and TBS=16. (b) $\pi/4$ -QPSK, and TBS=56.

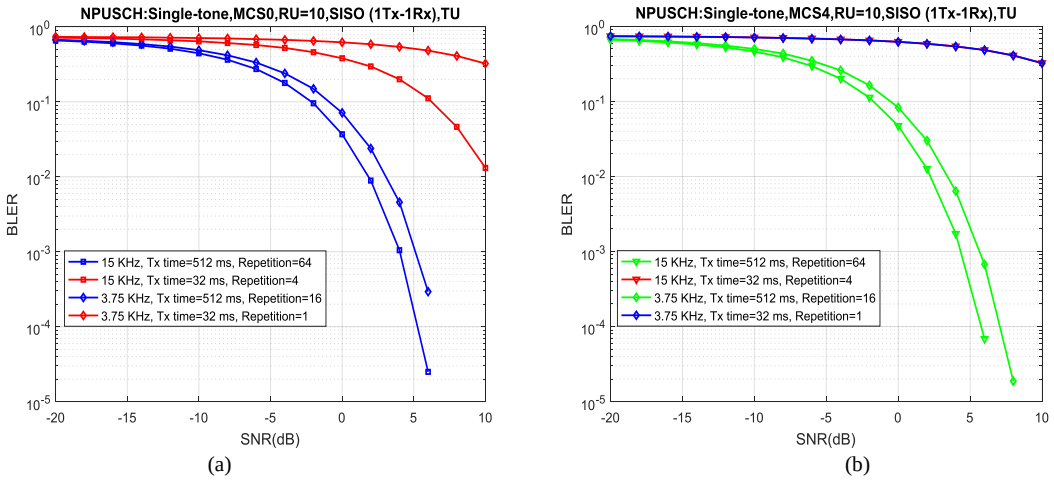

(a) (b)

Fig. 5. BLER performance of NPUSCH with single-tone transmission for both 15 KHz and 3.75 KHz subcarrier spacing using repetitions. Resource unit RU=10. (a) $\pi/2$ -BPSK , and TBS=256. (b) $\pi/4$ -QPSK, and TBS=680.

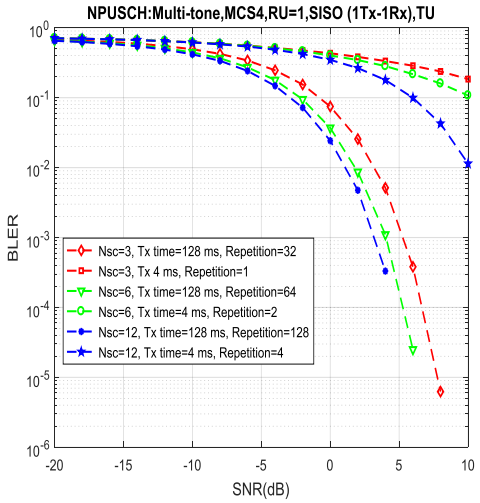

Fig. 6. BLER performance of NPUSCH for multi-tone transmission with QPSK modulation when TBS=56.

Moreover, the simulation curves in Fig. 7 show the relationship between repetition and received SNR for different numbers of resource unit. The results suggesting that with large number of repetitions up to 128, the transmit data block can be decoded even when the noise power is greater than the signal power. Finally, we conclude that user data can be transmitted in extremely bad radio conditions by utilizing signal repetition as well as our developed uplink system model is feasible to practical implementation of low-complexity NB-IoT systems.

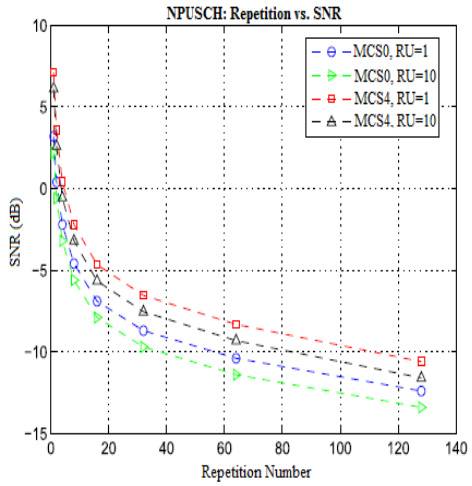

Fig. 7. Relationship curves between repetition number and receive SNR for NB-IoT uplink systems.

VI. Conclusion

In this paper, we provide a brief overview of NB-IoT systems and identify different parameters and operations required to evaluate the uplink coverage performance. An analytic repetition-dominated baseband signal model is derived for LTE-based NB-IoT uplink systems. A simple single-input single-output (SISO) system is considered for our analysis and investigation. Coverage performance is investigated for both single-tone and multi-tone transmissions. LS channel estimation and ZF equalization is performed in the receiver side which can be fit with low-complexity NB-IoT systems. Rigorous link-level computer simulations are provided to evaluate the coverage performance using signal repetition techniques. Our evaluations show that coverage performance can be significantly improved as with the large number of same signal repetitions. The coverage performance also depends on channel estimation quality. In the future, we will conduct channel estimation by means of noise power and channel covariance matrix and take into account the receive diversity for NB-IoT uplink systems performance analysis.

Acknowledgement

The authors would like to thank the Information Science Laboratory Center of University of Science and Technology of China (USTC) for hardware and software services. This research was supported by the National Natural Science Foundation of China (NSFC) under grant No. 61732020.

References

[1] Cellular networks for massive IoT-enabling low power wide area applications. (2016). Ericsson. [Online]. Available: https://www.ericsson.com/res/docs/whitepapers/wp_iot.pdf

[2] LTE evolution for IoT connectivity. (2016). Nokia. [Online]. Available: https://resources.ext.nokia.com/asset/200178

[3] A. D´ıaz-Zayas, C. A. Garc´ıa-Pe´rez, A. M. Recio-Pe´rez, and P. Merino, "3GPP standards to deliver LTE connectivity for IoT," in *Proc. IEEE 1st Int. Conf. on Internet-of-Things Design and Implementation (IoTDT)*, pp. 283-288, Apr. 2016.

[4] R. Want, B. N. Schilit, and S. Jenson, *Enabling the Internet of Things*, Published by IEEE Computer Society, pp. 28-35, 2015.

[5] A. Al-Fuqaha *et al.*, "Internet of Things: A survey on enabling technologies, protocols, and applications," *IEEE Communication Surveys and Tutorials*, vol. 17, no. 4, pp. 2347-2376, 2015.

[6] SigFox. [Online]. Available: https://www.sigfox.com/

[7] J. Pet äj äj ärvi, K. Mikhaylov, M. H ämäl äinen, and Iinatti, "Evaluation of LoRa LPWAN technology for remote health and wellbeing monitoring," in *Proc. 10th International Symposium on Medical Information and Communication Technology*, Mar. 2016, pp. 1-5.

[8] A. Rico-Alvarino, *et al.*, "An overview of 3GPP enhancements on machine to machine communications," *IEEE Comm. Mag.*, vol. 24, no. 6, pp. 14-21, June 2016.

[9] New Work Item: Narrowband IoT (NB-IoT). TSG RAN Meeting#69, 2015. 3GPP. [Online]. Available: www.3gpp.org/FTP/tsg_ran/ TSG_ RAN / TSGR_69/ Docs/RP-151621.zip

[10] R. Ratasuk, N. Mangalvedhe, Y. Zhang, M. Robert, and J. P. Koskinen, "Overview of Narrowband IoT in LTE Rel-13," in *Proc. of IEEE Conf. on Standards for Communications and Networking*, 2016.

[11] Y. P. E. Wang, *et al*., "A premier on 3GPP narrowband internet of things (NB-IoT)," *IEEE Com. Mag.* pp. 117-123, March 2017.
[12] New Study Item on Cellular System Support for Ultra Low Complexity and Low Throughput Internet of Things. TSG-GERAN Meeting #62, 2015. 3GPP. [Online]. Available: https://www.3gpp.org/ftp/tsg_geran/TSG_GERAN/GERAN_62Valencia/Docs/GP-140421.zip
[13] C. Yu, L. Yu, Y. Wu, Y. He, and Q. Lu, "Uplink scheduling and link adaptation for narrowband internet of things systems," *IEEE Access*, vol. 5, pp. 1724-1734, March 2017.
[14] L. Zhang, A. Ijaz, P. Xiao, and R. Tafazolli, "Channel equalization and interference analysis for uplink Narrowband Internet of Things (NB-IoT)," *IEEE Communications Letters*, vol. 21, no. 10, pp. 2206-2209, Oct. 2017.
[15] W. Yang, *et al*., "Enhanced system acquisition for NB-IoT," *IEEE Access*, vol. 5, pp. 13179-13191, July 2017.
[16] M. Lauridsen, H. Nguyen, B. Vejlgaard, I. Z. Kov ́acs ́, P. Mogensen, and M. Sørensen, "Coverage comparison of GPRS, NB-IoT, LoRa, and sigFox in a 7800 Km^2 area," in *Proc. IEEE Vehicular Technology Conference*, 2017.
[17] R. Ratasuk, N. Mangalvedhe, J. Kaikkonen, and M. Robert, "Data channel design and performance for LTE Narrowband IoT," in *Proc. IEEE Vehicular Technology Conference*, Sep. 2016.
[18] Y. D. Beyene, R. Jantti, K. Ruttik, and S. Iraji, "On the performance of Narrow-Band Internet of Things (IoT)," in *Proc. IEEE Wireless Communications and Networking Conference*, March 2017.
[19] A. Adhikary, X. Lin, and Y. P. E. Wang, "Performance evaluation of NB-IoT coverage," in *Proc. IEEE Vehicular Technology Conference*, Sep. 2016.
[20] N. Mangalvedhe, R. Ratasuk, and A. Ghosh, "NB-IoT deployment study for low power wide area cellular IoT," in *Proc. IEEE 27th Annual Symposium on Personal, Indoor, and Mobile Radio Communications (PIMRC) – Workshop: From M2M Communications to Internet of Things*, Sept. 2016.
[21] R. Ratasuk, B. Vejlgaard, N. Mangalvedhe, and A. Ghosh, "NB-IoT system for M2M communication," in *Proc. IEEE Wireless Communications and Networking Conference Workshops*, Apr. 2016.
[22] Evolved Universal Terrestrial Radio Access (E-UTRA); physical channels and modulation, 3GPP Tech. Spec. Group Radio Access Network, V 13.4.0, Rel. 13, Tech. Spec. TS 36.211. (2016). [Online]. Available: http://www.3gpp.org/ftp/Specs/archive/36_series/36.211/36211-d40 .zip
[23] Evolved Universal Terrestrial Radio Access (E-UTRA); physical layer procedures, 3GPP Tech. Spec. Group Radio Access Network, V 13.4.0, Rel. 13, Tech. Spec. TS 36.213, (2016). [Online]. Available: http://www.3gpp.org /ftp// Specs/archive/36_series/36.213/36213-d40.zip
[24] Evolved Universal Terrestrial Radio Access (E-UTRA); Multiplexing and channel coding, 3GPP Tech. Spec. Group Radio Access Network, V 13.4.0, Rel. 13, Tech. Spec. TS 36.212. (2016). [Online]. Available: http: //www.3gpp.org/ftp//Specs/archive/36_series/36.212/36212-d40.zip
[25] F. E. A. El-Samie, F. S. Al-kamali, Z. Y. Al-Nahari, and M. I. Dessouky, *SC-FDMA for Mobile Communications*, Boca Raton, FL, USA: CRC, 2013.
[26] Evolved Universal Terrestrial Radio Access (E-UTRA); User Equipment (UE) Radio Transmission and Reception, 3GPP Tech. Spec. V13.1, Rel. 13, Tech. Spec. TS36.101, Jan. 2017.
[27] Evolved Universal Terrestrial Radio Access (E-UTRA); User Equipment (UE) Conformance Specification; Radio Transmission and Reception, 3GPP Tech. Spec. V13.3.0, Rel. 13, Tech. Spec. TS36.521-1, Jun. 2016.

Md Sadek Ali was born in Kushtia, Khulna division, Bangladesh, in 1982. He received B.Sc. (Hon's) and M.Sc. degrees in Information and Communication Engineering from Islamic University, Kushtia-7003, Bangladesh in 2004 and 2005 respectively. He is now pursuing PhD degree in Micro-/Nano- Electronic System Integration R&D Center (MESIC) at the University of Science and Technology of China (USTC), Hefei, Anhui, 230026, PR China. He has authored or coauthored 10 Journal and 4 conference papers. His research interests include Physical layer of LTE, LPWAN technology, and NB-IoT.

Yu Li received the B.S. degree in Electrical Engineering from the University of Science and Technology of China, Hefei, Anhui, China, in 2013, and He is now pursuing PhD degree in Micro-/Nano- Electronic System Integration R&D Center at the University of Science and Technology of China, Hefei, Anhui, China. His research interests include parameter estimation, frequency and timing synchronization and NB-IoT cell search.

Song Chen received his B.S. degree in Computer Science from Xi'an Jiaotong University, China in 2000. Subsequently, he obtained a Ph.D. degree in Computer Science from Tsinghua University, China in 2005. He served at the Graduate School of Information, Production and Systems, Waseda University, Japan, as a Research Associate from August 2005 to March 2009 and as an Assistant Professor from April 2009 to August 2012.
He is currently an Associate Professor in the Department of Electronic Science and Technology, University of Science and Technology of China (USTC). His research interests include several aspects of VLSI design automation, on-chip communication system, and brain-inspired neuromorphic computing systems. He is a member of IEEE, ACM and IEICE.

Fujiang Lin received his B.S. and M.S. degrees from University of Science and Technology of China (USTC) in 1982 and 1985 respectively. In 1993, Lin received his Ph.D. from the University of Kassel, Germany. He currently works as a professor and doctoral supervisor at the School of Information Science and Technology, (USTC). He is also the Executive Director of the Department of Electronic Science and Technology, USTC.

He has long been engaged in cross-disciplinary research on microwave / microelectronics, being an influential scholar in this field internationally. Prof. Lin has served IEEE activities in different functions since 1995 including chair of the Singapore Microwave Theory and Techniques (MTT)/Antennas and Propagation (AP) Chapter, reviewer board member for the IEEE Microwave Theory and Techniques Society (MTT-S), and Technical Program Committee (TPC) member of RFIC. He is the initiator and co-organizer of series IEEE international symposium, workshops and short courses such as Radio-Frequency Integration Technology (RFIT). He was the recipient of the 1998 Innovator Award presented by EDN Asia Magazine. Prof. Lin has authored or coauthored over 100 scientific papers. He also jointly holds five patents.